

## ON THE NULLING, DRIFTING, AND THEIR INTERACTIONS IN PSRS J1741–0840 AND J1840–0840

GAJJAR, VISHAL<sup>1</sup>

Xinjiang Astronomical Observatory, CAS, 150 Science 1-Street, Urumqi, Xinjiang 830011, China  
Key Laboratory of Radio Astronomy, Chinese Academy of Sciences, Nanjing 210008, China  
Space Science Laboratory, 7–Gauss way, University of California, Berkeley 94710, USA

J. P. YUAN<sup>2</sup>, R. YUEN, Z. G. WEN, Z. Y. LIU, N. WANG

Xinjiang Astronomical Observatory, CAS, 150 Science 1-Street, Urumqi, Xinjiang 830011, China  
Key Laboratory of Radio Astronomy, Chinese Academy of Sciences, Nanjing 210008, China

<sup>1</sup>vishalg@berkeley.edu

<sup>2</sup>yuanjp@xao.ac.cn

### ABSTRACT

We report detailed investigation of nulling and drifting behavior of two pulsars PSRs J1741–0840 and J1840–0840 observed from the Giant Meterwave Radio Telescope at 625 MHz. PSR J1741–0840 was found to show nulling fraction (NF) of around  $30\pm 5\%$  while PSR J1840–0840 was shown to have NF of around  $50\pm 6\%$ . We measured drifting behavior from different profile components in PSR J1840–0840 for the first time with the leading component showing drifting with  $13.5\pm 0.7$  periods while the weak trailing component showed drifting of around  $18\pm 1$  periods. Large nulling do hamper accuracy of these quantities derived using standard Fourier techniques. A more accurate comparison was drawn from driftband slopes, measured after sub-pulse modeling. These measurements revealed interesting sporadic and irregular drifting behavior in both pulsars. We conclude that the previously reported different drifting periodicities in the trailing component of PSR J1741–0840 is likely due to the spread in these driftband slopes. We also find that both components of PSR J1840–0840 show similar driftband slopes within the uncertainties. Unique nulling–drifting interaction is identified in PSR J1840–0840 where, in most occasions, the pulsar tends to start nulling after what appears to be an end of a driftband. Similarly, when the pulsar switches back to an emission phase, in most occasions it starts at the beginning of a new driftband in both components. Such behaviors have not been detected in any other pulsars to our knowledge. We also found that PSR J1741–0840 seems to have no memory of its previous burst phase while PSR J1840–0840 clearly exhibits memory of its previous state even after longer nulls for both components. We discuss possible explanations for these intriguing nulling–drifting interactions seen in both pulsars based on various pulsar nulling models.

*Keywords:* pulsars, radio pulsars — pulsar nulling — pulsar drifting – PSR J1741–0840 – PSR J1840–0840

### 1. INTRODUCTION

Single pulses from some radio pulsars show remarkable phenomena, such as nulling, mode–changing, and sub–pulse drifting. Pulsar nulling has been shown to occur in around 100 pulsars to date (Ritchings 1976; Rankin 1986; Biggs 1992; Vivekanand 1995; Wang et al. 2007; Gajjar et al. 2012), with the phenomenon exhibits as an abrupt switch off in the the pulsed emission for a certain duration (hereafter: *null state*) (Backer 1970). The amount of null pulses, also quantified by the Nulling Fraction (NF)<sup>1</sup>, ranges from less than 1% to more than 95% (e.g. PSR J1717–4054; Wang et al. 2007 and PSR J1752+2359; Gajjar et al. 2014b). The nulls were also found to last for different durations ranging from just one or two seconds (e.g. PSR B0809+74; Ritchings 1976)

to many hours or even years (e.g. PSR J1832+0029; Camilo et al. 2012).

In many long-period pulsars, the consecutive sub–pulses in a sequence of single pulses (folded at the basic pulsar period  $P_1$ ) vary in phase or longitude systematically, forming apparent driftbands. The separation between driftbands where sub–pulses reappear at similar longitude, also known as drifting periodicity,  $P_3$ , varies from several to a few tens of  $P_1$ . The drift rate is defined as  $D = P_2/P_3$ , where  $P_2$  is the spacing between sub–pulses within a single pulse. Some pulsars are known to switch between different  $P_3$  modes. For example PSRs B0031–07 (Huguenin et al. 1970) and B2319+60 (Wright & Fowler 1981) exhibit three distinct values in the drift rates.

In a few pulsars, both nulling and drifting phenomena were

<sup>1</sup> NF represent fraction of null pulses in the data.

**Table 1.** Basic parameters of two pulsars

PSR	J1741–0840	J1840–0840
Period (sec)	2.043082	5.309377
DM (pc·cm <sup>-3</sup> )	74.90	272.00
RA (J2000)	17h41m22.5s	18h40m51.9s
DEC (J2000)	-08°40′31.9″	-08°40′29″
Age (Myr)	14.2	3.5
B <sub>s</sub> (×10 <sup>12</sup> G)	2.18	11.3
$\dot{E}$ (×10 <sup>30</sup> ergs/sec)	10.5	6.25

Note : Here, the DM represents dispersion measure while the RA and DEC are the right ascension and declination, respectively. The B<sub>s</sub> represents average surface magnetic field while the  $\dot{E}$  represents rate of loss-of-energy of the pulsar.

seen to co-exist and even shown to be interacting with each other. For example, PSRs B0809+74 and B0818–13 exhibit changes in the drift rate after the null states (Lyne & Ashworth 1983; van Leeuwen et al. 2003; Janssen & van Leeuwen 2004). During some of these interactions, the pulsars also seem to indicate some sort of phase memory in that information was retained regarding the phase of the last burst or active pulse during the null state. For example, PSR B0031–07 was shown to retain memory of its pre-null burst phase across short nulls (Vivekanand & Joshi 1997; Joshi & Vivekanand 2000). If both nulls and drift-mode changes are result of intrinsic changes in the pulsar magnetosphere, then their interactions could provide important clue for understanding the triggering and transition mechanism for changes between different magnetospheric states. Furthermore, evidences have been mounting to support a close relationship between nulling and drift-modes/profile-modes switching (Wang et al. 2007; Lyne et al. 2010; Cordes 2013; Hermsen et al. 2013; Gajjar et al. 2014b). It is likely that nulling in itself could be an extreme form of mode-changing where a pulsar switches between different magnetospheric states as indicated by recently reported broadband behavior of three nulling pulsars (Gajjar et al. 2014a). Thus, studies of pulsars that exhibit both nulling and drifting phenomena are essential in order to understand the true nature and origin of the nulling phenomenon. We present here observations of two pulsars, PSRs J1741–0840 and J1840–0840, which appear to show interactions between the nulling and drifting phenomena as hinted from the single pulses reported by Burke-Spolaor et al. (2012). However, these observations were not long enough to carry out detailed investigations of nulling and its interaction with the drifting phenomenon. Here, we report results for these pulsars from relatively longer observations, whose basic parameters are listed in Table 1.

PSR J1741–0840 (PSR B1738–08) was discovered during the earlier searches (Manchester et al. 1978) from the Molonglo telescope in Australia. It is a known drifting pulsar with a few studies (Weltevrede et al. 2006, 2007; Basu et al. 2016) reporting its abnormal drifting behavior. It displays two distinct profile components at 325 MHz. Weltevrede et al. (2006,

2007) have reported drifting phenomenon in this pulsar for the first time at 1420 MHz and 325 MHz, respectively. Weltevrede et al. (2007) hinted towards a possible nulling phenomenon in PSR J1741–0840, however, the length of their observation was not long enough to quantify the occurrence of nulls. To investigate nulling, drifting and their interaction further, we observed this pulsar for nearly two hours and obtained around 3095 single pulses. Weltevrede et al. (2006) have reported different P<sub>3</sub> values for the leading and the trailing components in this pulsar at 1400 MHz. The trailing component was reported to have P<sub>3</sub> of around 4.4±0.3 periods while the leading component has slightly slower drifting with P<sub>3</sub> of around 5.2±0.1 periods. The authors suggested that this difference in P<sub>3</sub> in the two components could be due to drift-mode switching. Weltevrede et al. (2006) have indicated that the trailing component might also have an additional drifting feature with P<sub>3</sub> of around 2 periods. Further observations at 300 MHz by Weltevrede et al. (2007) revealed two P<sub>3</sub> values of 4.8±0.1 and 4.7±0.1 periods which were not possible to separate between the two components due to the sensitivity of their observations. Moreover, Basu et al. (2016) have confirmed the 4.7±0.6 periods feature at 325 MHz and the 4.8±0.6 periods feature at 610 MHz. Here, we report its detailed behavior at 625 MHz with longer observations in contrast to Basu et al. (2016).

PSR J1840–0840 was discovered during the recent searches conducted from the Parkes telescope (Lorimer et al. 2006). Burke-Spolaor et al. (2012) reported short single pulse observation of this pulsar which pointed toward possible occurrence of nulling and drifting phenomena. The period of this pulsar is very large (~5.3 sec) giving around 1260 single pulses in our 2-hour observation. This pulsar exhibits two profile components at 610 MHz, which are located very close to each other. The leading component is slightly stronger in intensity than that of the trailing component. We are reporting here a unique nulling-drifting interaction in this pulsar for the first time.

The observations are discussed in Section 2 along with the descriptions on data recording and off-line data processing. The nulling behavior of both pulsars is discussed in Section 3 in which we discuss quasi-periodic feature found in PSR J1741–0840. Single pulse drifting results are discussed in Section 4. A modeling of driftbands is discussed in Section 5 which is essential to determine changes in the drifting pattern. We discuss null associated changes in these drift rates in Section 5.1, while the phase memory across the nulls is discussed in Section 6 for both pulsars. The final conclusion and implication of our findings are discussed in the Section 7.

## 2. OBSERVATIONS

The observations were conducted using the Giant Meter-wave Radio Telescope (Swarup et al. 1991) on 19th January, 2013. The GMRT correlator was used as a digital filterbank to obtain 512 spectral channels, each having a bandwidth of 62.5

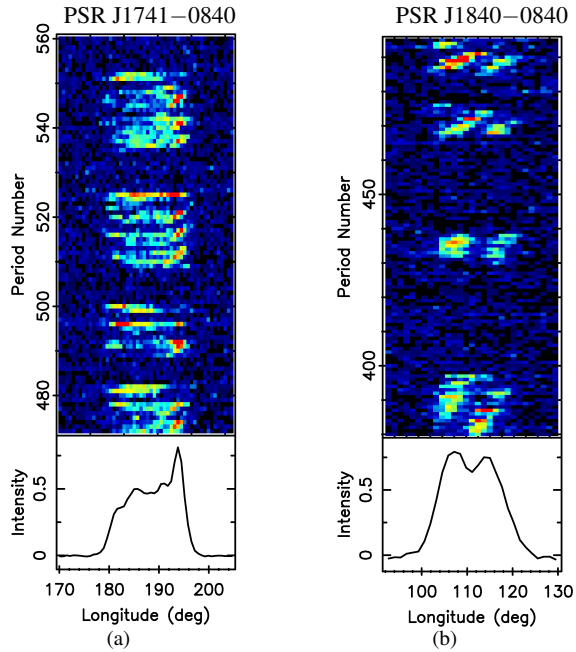


**Figure 1.** Sections of single pulses for the two pulsars observed at 625 MHz from the GMRT. The top panel shows a section of observed pulses while the bottom panel shows the integrated profile from the entire observation for each pulsar. (a) PSR J1741–0840 shows prominent nulls separated by burst bunches which exhibit clear sub-pulse drifting in the trailing component, (b) PSR J1840–0840 exhibit prominent long and short nulls along with prominent drifting during the short burst phases.

KHz across the 32 MHz bandpass received for each polarization from each GMRT antenna. The digitized signals from the 14 GMRT antennas were added in phase to form a coherent sum of signals with the GMRT Array Combiner (GAC) (Prabhu 1997). Then, the summed signals were detected in each channel of each polarization. The detected power in each channel were then acquired into 16-bit register every  $122.88\mu\text{s}$  after summing the two polarizations in a digital backend and were accumulated before being written to an output buffer to reduce the data volume. The data were then acquired using a data acquisition card and recorded to a tape-drive for the off-line processing.

In the off-line processing, the raw filterbank data were first processed to handle spurious radio frequency interferences (RFI). We have deployed a similar method as suggested by Hotan et al. (2004) and van Straten et al. (2012) to remove time-domain and frequency-domain RFI from the raw GMRT filterbank data. We first determined median from 512 frequency channels for each time sample. Channels which exhibit three times more power than the median value were identified and replaced with the measured median value for a given time sample. For the time-domain RFI excision, we first calculated number of samples corresponding to the period of the pulsar in a given file. We calculated average power by adding

all frequency channels for each sample. Samples that exhibited powers larger than three times the median value were replaced with a combination of a median and Gaussian noise equivalent to the standard deviation of the data. In order to keep the sensitivity similar for each observed pulse, similar number of samples were replaced for each period. For each block – of number of samples per period and number of frequency channel per sample – only top 20% of the *bad* data were replaced. The raw GMRT filterbank data were then converted to SIGPROC<sup>2</sup> (Lorimer 2001) filterbank format. We used standard SIGPROC dedispersion and folding tool to produce single pulses for further analysis of each pulsar. The data were folded to 512 or 1024 phase bins across the topocentric pulse period to obtain the single pulse sequences. It should be noted that although excision of RFI from the raw filterbank data improved the S/N for the observed single pulses, there were a few pulses which showed clear presence of RFI and hence removed entirely for the nulling fraction (NF) analysis of both the pulsars.

### 3. NULLING

We report here the NF for both pulsars for the first time. Figure 1 shows a section of the observed single pulses, in which the pulses with no detectable emission are clearly visible from the two pulsars. It should be noted from Figure 1(a) that – unlike profile at 325 MHz (Weltevrede et al. 2007) – PSR J1741–0840 does not exhibit two distinct profile components at 625 MHz. Prominent nulling along with regular drifting in two components can be seen for PSR J1840–0840. Figure 1(b) also shows an example of occasional long null of around 27 periods in PSR J1840–0840. The NFs for both pulsars were obtained using a procedure similar to that used for detecting pulse nulling from the single pulse sequences by Gajjar et al. (2012). We obtained the on-pulse and off-pulse energy histograms using appropriate on-pulse and off-pulse windows of similar length. Figure 2 shows these histograms with prominent nulls located near the zero pulsed energy for both pulsars. In Figure 2 the on-pulse energy histograms show clear bi-modal distributions that point toward two separate populations each belonging to null and burst pulses for both pulsars. A Gaussian function was fitted for both the on-pulse and off-pulse histograms for each pulsar. A ratio between the peaks of on-pulse and off-pulse histograms provides estimation of NF<sup>3</sup> for a given pulsar. The estimated NF for PSR J1741–0840 is around  $30\pm 5\%$  while the estimated NF ( $50\pm 6\%$ ) for PSR J1840–0840 suggests that around half the observed pulses are likely to be nulls. The larger error bars are due to weak burst pulses which do hinder a clear distinction between these populations.

It is essential to confirm that the observed nulls are true

<sup>2</sup> <http://sigproc.sourceforge.net>

<sup>3</sup> Although Gajjar et al. (2012) have demonstrated that the NF is not an ideal parameter to quantify nulling, we are reporting them here for the sake of comparison.

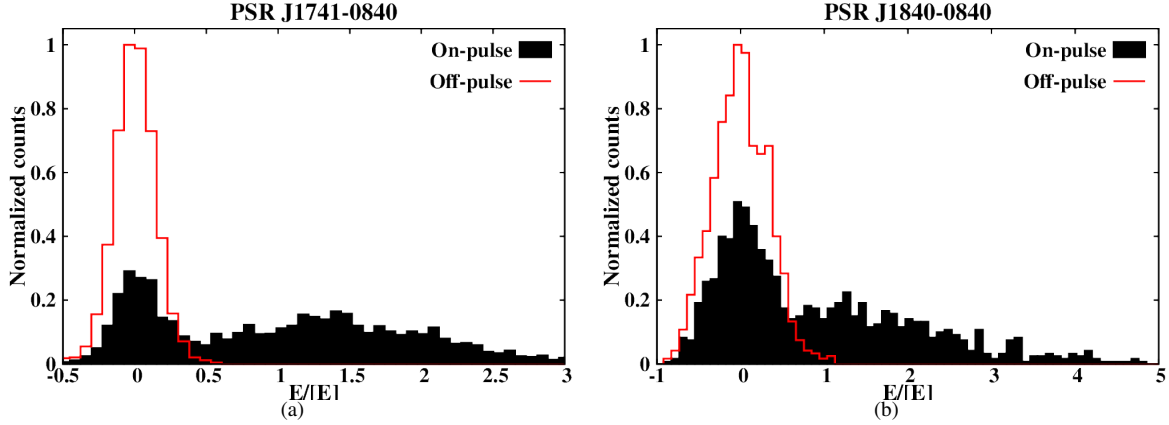


**Figure 2.** The on-pulse and off-pulse energy histograms for the two pulsars observed from the GMRT at 625 MHz. The red solid line indicates off-pulse histograms while the black fill regions are the on-pulse energy histograms. (a) PSR J1741–0840 shows very clear nulling with a distinctly separate null and burst pulses among the on-pulse energy distribution. The estimated NF for this pulsar is around  $30 \pm 5\%$ . (b) PSR J1840–0840 exhibits large fraction of null pulses, with NF of around  $50 \pm 6\%$ , which can also be noticed from the large distribution of pulses around zero pulse energy.

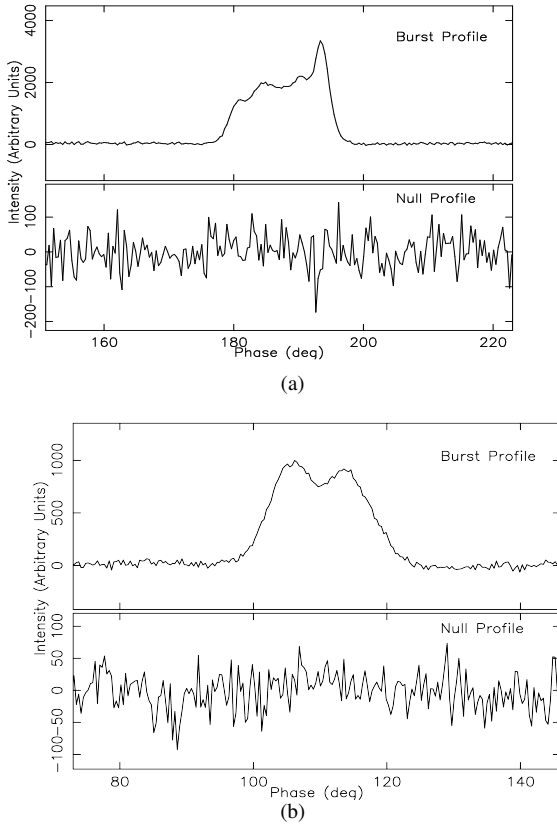


**Figure 3.** The integrated profile obtained separately for null and burst pulses for (a) PSR J1741–0840 and (b) PSR J1840–0840. The top panel shows profile from the burst pulses only and the bottom panel shows average profile after combining only null pulses for respective pulsars. The null profile does not show any detectable profile component, suggesting absence of any weak level emission.

nulls and are not just weak emission phases where emission from the single pulses goes below the detection threshold of the telescope. For example, PSRs B0826–34 and B0823+26 were reported to show weak emission in the previously reported nulls (Esamdin et al. 2005; Sobey et al. 2015). We separated all the nulls from the burst pulses using a method described in Gajjar et al. (2012, 2014b) for both pulsars. A weighted sum was performed over all on-pulse bins for each observed pulses using the shape of their integrated pulse profile. For each pulsar, all the observed pulses were arranged in the ascending order of their weighted pulse energy. A threshold was moved from the high energy end towards the low energy end until pulses below this threshold did not show a significant profile component ( $< 3\sigma$ ). This threshold was used to divide all pulses into two groups with pulses below the threshold marked as nulls and pulses above the threshold marked as bursts. A visual inspection was also carried out on all the separated null pulses and most of the mislabeled burst pulses were removed and added to the burst pulse group. Figure 3 confirms that these nulls clearly show absence of any detectable emission for all components in both pulsars.

### 3.1. Quasi-periodic fluctuations

The separated null and burst pulses were again arranged in the order they were observed for each pulsar. It should be noted that as both pulsars exhibit multiple profile components, we consider complete absence of emission for all components as the beginning of a null state. The length of contiguous emission states (in any profile component) were measured and labeled as *burst-lengths* and separation between these bursts were measured as *null-lengths*. For PSR J1741–0840, as shown in Figure 4(a), the burst-lengths clearly shows a good fraction of burst bunches with 25 to 30 periods while the null-lengths tends to show cluster between 5 to 10 periods. PSR

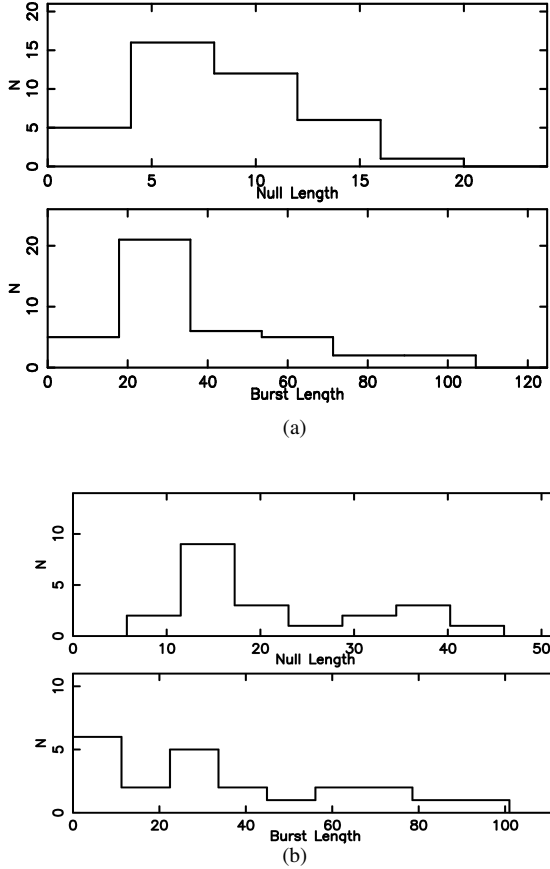


**Figure 4.** The null-length and burst-length distributions for (a) PSR J1741–0840 and (b) PSR J1840–0840. The top panel shows distribution of length of observed nulls while the bottom panel shows distribution of observed consecutive burst pulses for corresponding pulsars. PSR J1741–0840 shows excess of around 30 period bursts corresponding to quasi-periodic feature seen from the burst bunches. For PSR J1840–0840 an excess can be seen around null lengths of 13 to 15 periods.

J1840–0840 shows clustering at null length of around 13 to 15 periods while the burst length seems to have short bursts along with bunches around 25 to 30 periods. In earlier studies, a few nulling pulsars were known to show such clustering (Rankin & Wright 2008; Gajjar et al. 2014b), which could give rise to quasi-periodic pulse energy fluctuations.

As evident from Figure 1(a), the single pulses from PSR J1741–0840 can also clearly be seen to switch quasi-periodically between the null and burst states which can be investigated further by taking a Fourier transform of the pulse energy modulation. Such bunching of burst and null pulses will give rise to periodic feature in the on-pulse energy fluctuation spectra, especially at lower fluctuation frequencies. Weltevrede et al. (2007) have also reported a low frequency excess in their fluctuation spectra for PSR J1741–0840, however, no measurements was reported with possible quasi-

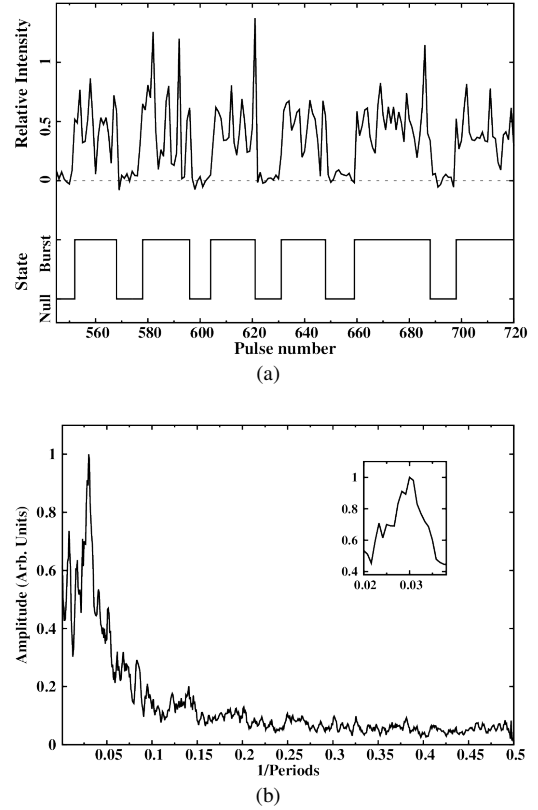


**Figure 5.** Quasi-periodic fluctuations in the pulse energy of PSR J1741–0840 at 625 MHz. (a) The top panel shows the pulse energy modulation as a function of observed period. The bottom panel shows the identified emission state (null or burst) corresponding to each period. (b) Fourier spectrum of the pulse energy modulation pattern which clearly indicates strong periodicity. The inset plot displays the zoom in on the strong spectral feature which indicates periodicity of  $33 \pm 4$  periods.

periodicity of burst bunching. In more recent study, Basu et al. (2016) conducted observations of PSR J1741–0840 and reported drifting periodicities at 325 MHz and 610 MHz. Among the reported drifting features, low frequency periodic components were also reported with  $0.033 \pm 0.006$  cycles/ $P_1$  and  $0.033 \pm 0.009$  cycles/ $P_1$  at 325 MHz and 610 MHz, respectively. These low frequency drifting features correspond to roughly 30-period quasi-periodicity which is likely to come from the bunching of null and burst pulses. For PSR J1840–0840, no indication of quasi-periodicity were reported in the previous studies.

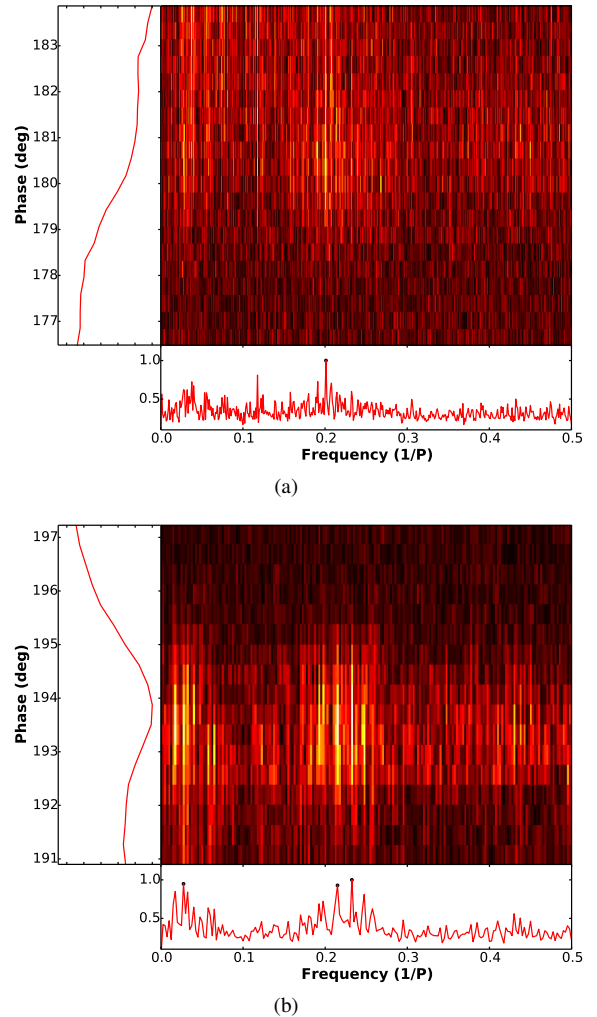
In order to measure this quasi-periodicity for the burst bunches, all the burst pulses were marked as ones and all remaining pulses (nulls) were marked as zeros for both pulsars. This one-zero sequence indicate emission state of the pulsar at each period, as shown in Figure 5(a). For PSR J1741–0840, it should be noted that a few burst bunches exhibit a small number of nulls, lasting for one or two periods, inside them. Similarly, a few nulls between the burst bunches also exhibit sin-

gle individual burst pulses. As we are interested in the quasi-periodicity of the burst bunches, these pulses were ignored in the one-zero sequence. A Fourier transform was carried out on this one-zero sequence to quantify the quasi-periodic pattern for both pulsars. As suggested by Herfindal & Rankin (2007, 2009), such technique helps in eliminating the pulse-to-pulse amplitude modulations and points toward exclusive modulation of the burst bunching. Figure 5(b) shows the spectrum with a clear quasi-periodic feature around  $33 \pm 4$  periods for PSR J1741–0840. This periodicity also matches with the bunches seen in the null length and burst length histograms shown in Figure 4(a). Thus, these measurements confirm that PSR J1741–0840 exhibits clear quasi-periodic burst bunches. We did not find any strong feature in the similar spectrum for PSR J1840–0840 (not shown here). It is also likely that the absence of any periodic pattern in PSR J1840–0840 could be due to large NF in our comparatively small number of observed pulses.

#### 4. PULSE ENERGY MODULATIONS

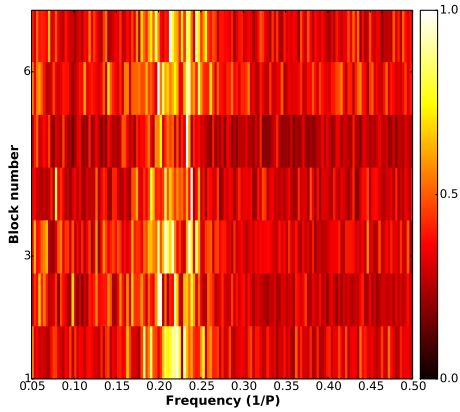
A visual inspection of single pulses from PSR J1741–0840 (Figure 1(a)) clearly shows driftbands in the trailing component while the leading component does not show such distinctive driftbands. This is consistent with the reported behavior by Weltevrede et al. (2006, 2007) at 1420 MHz and 325 MHz, respectively. We are unable to find any driftbands in the leading component, which indicates that any drifting periodicity seen in the component is likely to originate from possible amplitude modulation. Drifting in both components of PSR J1840–0840 is evident from Figure 1(b) but has never been reported in any previous studies. Although driftbands are prominent for both pulsars, the large NFs make the measurement of the drifting periodicity a challenging task. In order to estimate  $P_3$ , we measured the longitude-resolved fluctuation spectra (LRFS) for both pulsars. Collectively, the LRFS represents a Fourier transform computed over each individual phase bin, and can be represented in a 2-Dimensional contour plot along with average fluctuations taken over both axes. The pulsar period is first divided into 1024 phase bins for a given pulsar. A pulse-to-pulse fluctuation time-series is obtained for individual phase bin and a discrete Fourier transform is carried out over each of them to identify the fluctuation periodicities.

Figure 6 shows the spectra obtained for the leading and the trailing components of PSR J1741–0840. It should be noted that as PSR J1741–0840 exhibit quasi-periodic fluctuation of around 33 periods due to burst bunches (see section 3.1), thus the spectra obtained over a sequence containing nulls will be dominated by this quasi-periodic feature, as reported by earlier studies (Weltevrede et al. 2007; Basu et al. 2016). Such low frequency excess can be seen for both the components in Figure 6. The LRFS for the individual component suggests an interesting drifting behavior for this pulsar. The leading component shows a significant peak around  $4.9 \pm 0.1$  periods along



**Figure 6.** Longitude resolved fluctuations (LRFs) spectra of (a) leading component, and (b) trailing component of PSR J1741–0840 at 625 MHz. The abscissa is the frequency of the drifting periodicity and the ordinate is the profile phase for all three LRFs. The intensity of the drifting periodicities as a function of pulse phase is plotted in color contours. The leading component shows a modulation periodicity of  $4.9 \pm 0.1$  periods while the trailing component shows two distinct periodicities of around  $4.6 \pm 0.2$  and  $4.3 \pm 0.1$ . We fitted Gaussian functions at the center of these spectral lines and measured their widths to estimate errors with 90% confidence limit on the observed lines in the spectra.

with its harmonics. The trailing component, which has width of around  $6^\circ \pm 0.5^\circ$ , exhibits different degrees of periodicities with a prominent and relatively narrow peak around  $4.3 \pm 0.1$  periods, and a relatively broader peak around  $4.6 \pm 0.2$  periods. These dual periodicities are intriguing and require a closer and detail look at the drifting behavior in the trailing component. It can be speculated that these periodicities are not likely to be similar for all burst pulses. As mentioned in Section 1, a few pulsars exhibit time dependent drifting periodicities and switch between different drift modes. In order to



**Figure 7.** The LRF spectra of the trailing component of PSR J1741–0840 at 325 MHz from consecutive and overlapping block of 356 pulses with total 2206 single pulses. Most of the blocks show diffuse periodicities without any significantly prominent component.

scrutinize these drift modes, we computed a time-dependent LRFS for the trailing component. We first divided the observed sequence of 1206 pulses into 7 overlapping blocks, with each block consisting of 356 pulses. We then measured LRFS from each of the consecutive and overlapping blocks. The result is shown in Figure 7, which clearly exhibits broad and diffuse spectra for all the blocks implying similar drifting features in each block without any significant differences. It should be noted that  $P_3$  measured from the LRFS are averaged values which requires substantial number of periods with similar repeating pattern. As we are seeing multiple  $P_3$  peaks for each block, it is likely that drifting might be changing during the course of a single block of 356 periods considered here. Such rapid changes in the drifting periodicities, occurring on a smaller scale, might be possible to visually see from the drift-band slopes. We will explore a detailed analysis of the drift band slope changes in Section 5.

For PSR J1840–0840, the obtained LRFS for the leading and trailing components are shown in Figures 8(a) and 8(b), respectively. The leading component has width of around  $11 \pm 0.5^\circ$  and shows relatively stronger and broader peak of around  $13.5 \pm 0.7$  periods, as seen in Figure 8(a). A visual examination of the observed single pulses reveals that this periodicity is not stable and exhibits a range of driftband shapes. These changes are further quantified in Section 5. The trailing component of this pulsar has width of around  $9^\circ \pm 0.5^\circ$  and an estimated  $P_3$  of around  $18 \pm 1$  periods. Moreover, it can be seen from Figure 8(b) that the significance of  $P_3$  is relatively low compared to the  $P_3$  of the leading component. It should be noted that leading component shows slightly lower  $P_3$  compared to the trailing component. Such slight differences in  $P_3$  periodicity between different components are seen in a few pulsars in earlier studies. For example, PSR B0826–34 showed different  $P_3$  for different profile components (Biggs et al. 1985). However, it should be noted that as the pulsar ex-

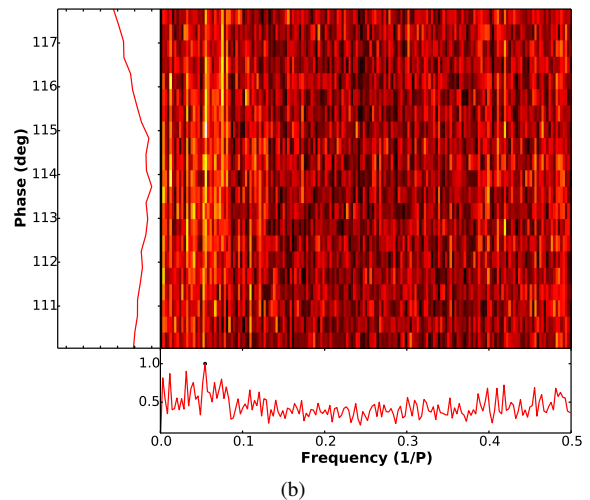
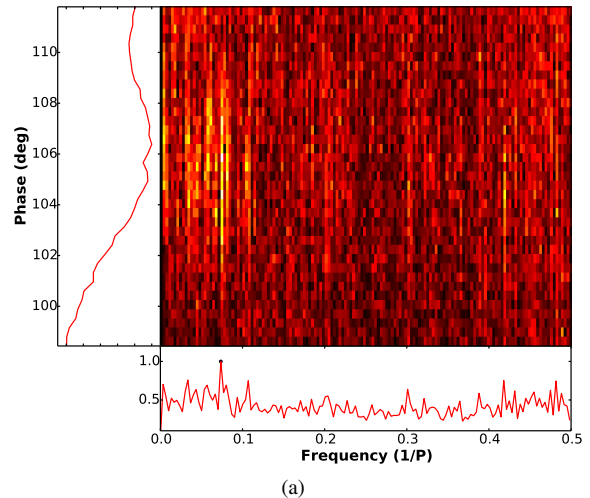


**Figure 8.** The longitude resolve fluctuation spectra of PSR J1840–0840 at 625 MHz for (a) the leading component and (b) trailing component. The notation for each axis is similar to Figure 6. The leading component exhibits drifting of around  $13.5 \pm 0.7$  periods while the trailing component exhibits longer periodicity of around  $18 \pm 1$  periods. As this pulsar exhibits longer sequence of null pulses, we were only able to identify a single sequence of 350 consecutive pulses which has relatively lower number of intervening long nulls. However, it should also be noted that these measurements are likely to be influenced by these intervening nulls.

hibits longer nulling instances, our  $P_3$  measurements, which were made from only a single sequence of around 350 consecutive pulses, is likely to be hampered by these intervening nulls. A more detailed comparison using the driftband slopes is required to scrutinize these differences of drifting between both components of PSR J1840–0840.

## 5. DRIFTBAND SLOPES

The spread in the driftband slope (hereafter drift-rate;  $D$ ) can point towards possible drift mode changes which can occur on a smaller time-scale compared to number periods re-

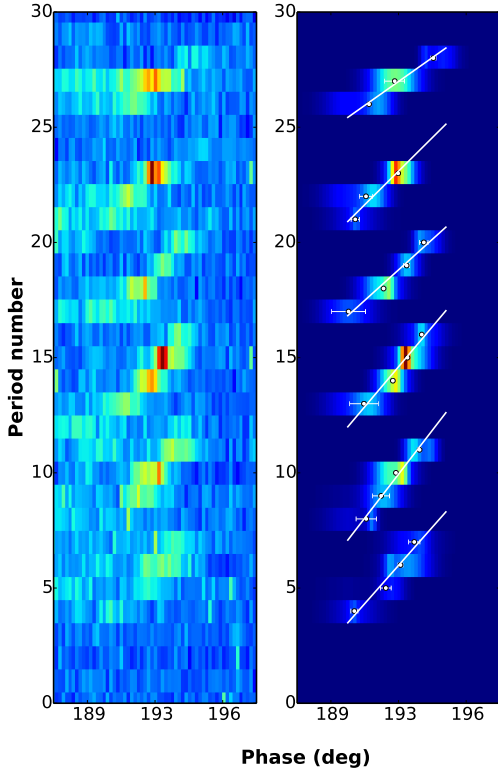


**Figure 9.** A section of the observed drifting in the trailing component of PSR J1741–0840 at 625 MHz is shown in the left plot. The corresponding Gaussian modeled components, along with the best linear fits (white straight lines) for each driftband, are shown in the right plot.

quired to measure the average  $P_3$ . If there are stable and distinct drift modes in a given pulsar, the measurements of  $D$  are likely to show some clustering corresponding to these modes. It should be noted that as  $D$  is a ratio between two quantities ( $D = P_2/P_3$ ), there is an inherent degeneracy regarding which parameter dominates that causes  $D$  to change. In other words, a similar fluctuations in sub-pulse separation ( $P_2$ ) can also make corresponding changes in the  $D$ . However, [Weltevrede et al. \(2007\)](#) have carried out study of a few hundred pulsars and concluded that  $P_2$  does not change during different drift modes. Moreover, a few earlier studies have also suggested stability of  $P_2$  ([Huguenin et al. 1970](#); [Taylor et al. 1975](#); [Lyne & Ashworth 1983](#)) in different pulsars. Thus, treating  $P_2$  as a constant for both pulsars allows us to assume that any significantly different values exhibited in  $D$  corresponds to different  $P_3$  measurements. We have used this same assumption in Sections 6 and 7.

In order to measure  $D$  with high significance, we modeled each single pulse from a given component – trailing for PSR J1741–0840 and both components for PSR J1840–0840 – using a Gaussian function for both pulsars. Such modeling has been carried out for many pulsars in earlier studies ([Lyne & Ashworth 1983](#); [Vivekanand & Joshi 1997](#); [Vivekanand & Joshi 1999](#); [van Leeuwen et al. 2002](#)). It provides unique

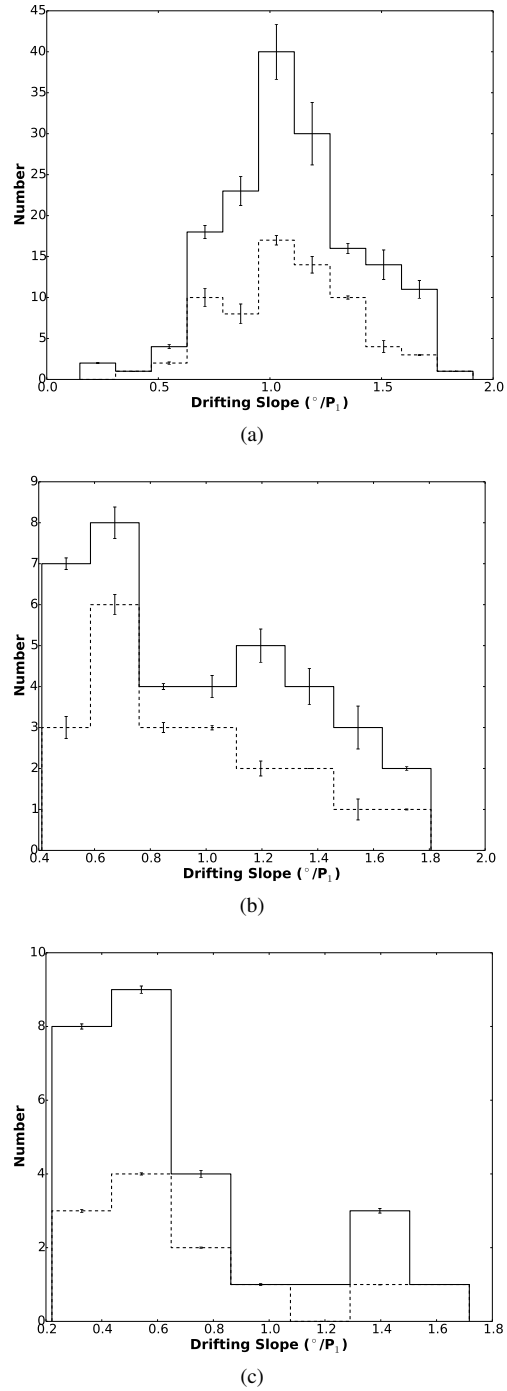


**Figure 10.** Histograms of measured drift-rates in (a) trailing component of the PSR J1741–0840, (b) leading, and (c) trailing components of PSR J1840–0840 at 625 MHz. The histograms with dotted line represent the drift-rates measured from the drift-bands around nulls. The error bars are obtained for each bin incorporating errors from the measured  $D$  in corresponding histogram bin. Both pulsars show no significant difference between the average drift-rates and the drift-rates measure around nulls.



smoothness to the true shape of the single pulse components, which is helpful in determining the drift-rate and its associated changes. Each component of every burst pulse was carefully modeled with a Gaussian function in order to keep the reduce Chi-square close to unity. Then, each fitted model sub-pulse was carefully examined visually to verify its representation of the true shape of the component under consideration. This modeling gives a center point for each sub-pulse which can be traced by fitting a straight line across a given driftband to determine the corresponding  $D$ . Figure 9 shows an example of several driftbands in the trailing component for a section of burst bunch from PSR J1741–0840. To determine the slope of these lines, individual errors in the estimation of modeled centers were also incorporated. Thus it was possible to obtain a more accurate estimation (with acceptable reduced Chi-square) of the slope with more stringent error only for driftbands with sufficient number of sub-pulses. For weak sub-pulses, the error bars on the estimated centers were relatively larger which propagated during the estimation of the driftband slopes, resulting in larger uncertainties. Figure 10 shows distribution of  $D$  obtained for both pulsars for corresponding components.

For PSR J1741–0840, distribution of the measured drift-rates (shown in Figure 10(a)) displays a large spread corresponding to driftbands with different slopes. The mean value of the measured  $D$  ( $\hat{D}$ ) is around  $1.1^\circ \pm 0.2^\circ / P_1$ , which was obtained from around 160 observed driftbands in the trailing component of PSR J1741–0840. It should be noted that the error bar on the measured  $D$  is large enough to produce different drifting periodicities seen in the LRFS given a relatively constant  $P_2$ . Although the  $D$  shows large spreads, we do not notice any significant clustering that could point to the presence of different drift modes. Thus, we did not identify any drift-modes in this pulsar which could explain the different  $P_3$  periodicities seen in the LRFS. It can be speculated that, the drifting is very sporadic and it changes irregularly without clearly producing distinguishable drift modes. Such changes can also be seen towards the last pulses in Figure 9 for PSR J1741–0840.

Figures 10(b) and 10(c) show distributions of  $D$  for PSR J1840–0840 which also exhibit significant spreads for both components. Since PSR J1840–0840 exhibits large fraction of null pulses, we identify only 37 and 27 significant driftbands for measurement of their slopes with good Chi-square fits in the leading and trailing components, respectively. From Figure 10(b) it can be speculated that the  $D$  has bi-modal distributions as indicated by the two peaks. The drift rate of the trailing component, shown in Figure 10(c), does show similar drift rates to the leading component although the number of good driftbands are relatively lesser. In order to scrutinize this bi-modality in  $D$  for both components, we carried out *Hartigan's Dip Test for Unimodality* proposed by [Hartigan & Hartigan \(1985\)](#). The test assumes a null hypothesis of unimodal distribution and provides a  $p$ -value for a given input samples.

We found that the  $p$ -value for unimodal distribution hypothesis is 93% and 95% for the leading and trailing components, respectively, which clearly suggest that the distribution of  $D$  is most likely to be unimodal for both components. It should be noted that our sample size was not sufficient enough (specially for the trailing component) to clearly claim bi-modality in Figures 10(b) and 10(c) with high significance. We simulated around 20,000  $D$  values for each components using Monte-Carlo technique and carried out the *Dip test* again but did not find any significant changes in the  $p$ -value. Thus, considering unimodal distribution of  $D$  we estimated average  $\hat{D}_l$  of around  $0.9^\circ \pm 0.4^\circ / P_1$  and  $\hat{D}_t$  of around  $0.7^\circ \pm 0.4^\circ / P_1$ , for the leading and trailing components, respectively. The  $\hat{D}_t$  is comparable to  $\hat{D}_l$  within error bars, which suggests that both components exhibit similar drifting periodicity that was not possible to scrutinize from the measurements of  $P_3$  in the individual component due to large nulling instances (see Section 4). Thus, it should be noted that such large spread in drift-rates can contribute to the broad and different  $P_3$  periodicities seen in both components of PSR J1840–0840 given a constant  $P_2$ .

Furthermore, we did not find any correlation between  $D$  and pulse-to-pulse intensity fluctuations to hint at any association between them. As both pulsars clearly show large fraction of nulls, it is likely that these nulls might be interacting significantly with these drift rates. This is discussed further in the next section.

### 5.1. Null associated drift rate changes

Nulls are known to cause significant changes in the drifting behavior of the adjacent burst pulses for a few pulsars ([Lyne & Ashworth 1983](#); [Deich et al. 1986](#); [Vivekanand & Joshi 1997](#); [Joshi & Vivekanand 2000](#); [van Leeuwen et al. 2002](#)). The burst pulses occurring before or after a null phase are known to show noticeable changes in the drifting slopes like that in PSR B0809+74 ([Lyne & Ashworth 1983](#); [van Leeuwen et al. 2002](#)) or it could also act as a trigger to cause a pulsar to switch between different drift-modes like in the case of PSR J1727–2739 ([Wen et al. 2016](#)). In order to investigate any changes in the drift slopes caused by nulls, we separated all the driftbands occurring before and after the null states for both pulsars.

For PSR J1741–0840, driftbands before the onset of nulls showed mean  $D$  ( $\hat{D}_b$ ) of around  $1.12^\circ \pm 0.2^\circ / P_1$  while the driftbands after the nulls showed mean  $D$  ( $\hat{D}_a$ ) of around  $1.05^\circ \pm 0.2^\circ / P_1$ . These are not significantly different from the  $\hat{D}$  measured from all driftbands. Similarly, for PSR J1840–0840 we separated all the driftbands around the nulls for both components. We only used driftbands which had sufficient S/N and provided good fit to the straight line tracing of its drifting direction. We found  $\hat{D}_{la}$  for the driftbands after the null states to be around  $0.97^\circ \pm 0.21^\circ / P_1$  and  $\hat{D}_{lb}$  for the driftbands before the onset of nulls is  $0.93^\circ \pm 0.27^\circ / P_1$  for the leading component. These measurements match with the

average value ( $\hat{D}_l$ ) within the error bars. For the trailing component, we found  $\hat{D}_{tb}$  and  $\hat{D}_{ta}$  to be around  $0.73^\circ \pm 0.54^\circ / P_1$  and  $0.64^\circ \pm 0.21^\circ / P_1$  for drift-rates before and after the nulls, respectively. These are also not significantly different from the  $\hat{D}_l$ . Figure 10 shows a separate distribution of measured  $D$  around nulls for both pulsars. As the driftbands do not show significantly different distributions, we conclude that none of the components exhibit noticeable driftband slope changes influenced by nulls.

## 6. DRIFTING PHASE MEMORY ACROSS NULLS

In a very few nulling pulsars, drifting seems to retain some memory of its phase from before the pulsar goes into a null state. Such memory may provide important link in understanding the true nature of the nulling phenomenon. We discuss two ways in which this phase memory across nulls can be scrutinized.

### 6.1. Turn-on and Turn-off phase preference

Joshi & Vivekanand (2000) suggested a comparison between the turn-off phase and the turn-on phase to investigate phase memory across nulls. In our case, these phases correspond to the center of each fitted Gaussian components of the burst pulses at the null-to-burst and burst-to-null transition instances. If a pulsar prefers particular phase during the transitions, last burst pulse before the null and first burst pulse after the null should exhibit distribution of phases significantly different from the average center for a given component. We obtained distributions of the turn-off phases ( $\phi_{off}$ ) and turn-on phases ( $\phi_{on}$ ) for the corresponding components in both pulsars. It should be noted that when calculating a first pulse after the null and last pulse before the null, we only consider emission in the component under consideration. Both components in both pulsars tend to show simultaneous transition instances with a very few exceptions and we assume that our outcome is not likely to get much influenced by these small discrepancies.

We did not find any preferences for the turn-off and turn-on phases for the trailing component of PSR J1741–0840 (see Figure 11(a)). Thus, it can be speculated that PSR J1741–0840 does not prefer any particular turn-on or turn-off phase around the null instances for its trailing component. We should point out that this non-correlation between the turn-on and turn-off phases can also be due to shorter drifting periodicity. Given a  $P_3$  of around 4.3 and 4.6 periods, in a complete cycle of a driftband we are only going to sample the sub-pulse phase 4 to 5 times. This can influence a correct measurement of turn-on and turn-off phases for around 25% of the time either way. Since we only study this behavior for only 12 transitions, our sample size is limited to rule it out entirely.

PSR J1840–0840 was seen to have a very strong preference for turn-on and turn-off phases for both components. Figures 12(a) and 13(a) highlight preferred localization of  $\phi_{on}$

and  $\phi_{off}$  from the histogram of their measured distributions for leading and trailing components, respectively. The average turn-on phase for the leading component was found to be around  $103.9 \pm 0.2$  which is significantly different from the average turn-off phase of around  $106.9 \pm 0.1$ . Similarly, the trailing component showed average turn-on phase of around  $113.2 \pm 0.3$  which is also noticeably different from the turn-off phase of around  $117.7 \pm 0.2$ . A Kolmogorov-Smirnov (KS) test of comparison between these distributions for both components rejected the null hypothesis of similarity with 99.9% probability (with KS-test  $D$  value of 0.76 for leading component and 0.84 for the trailing component), suggesting that these distributions are very distinct.

Thus, it is likely that both components of PSR J1840–0840 exhibit preferred localization for the turn-on and turn-off phases. In other words, it appears that nulls always start after completion of a full driftband and it is very likely to end with a beginning of a new driftband in either components. These results also suggest that typical burst durations are integer multiple of  $P_3$  periodicities which can be seen from Figure 4(b) with peaks around 15, 30 and 60 periods. Also typical bursts with around 15 periods for the leading and trailing components can also be seen in Figures 14(b) and 1(b). A few other examples of null instances along with preferred turn-on phase can also be seen from single pulses in Figure 1(b). This has never been seen with such high significance in any pulsars to the best of our knowledge.

### 6.2. Drifting across nulls

In this section we attempt to scrutinize motion or displacement of sub-pulses during the null states. As an extreme scenario, if drifting completely halts during nulls and the pulsar retains its phase memory, the turn-on phase is likely to be similar to the turn-off phase. In order to test this scenario for PSR J1741–0840, which exhibits range of turn-on and turn-off phases, we measured a correlation co-efficient between them. If turn-on and turn-off phases have any association across nulls, we are likely to see significant amount of correlation between them. We only compared those transitions where burst pulses – near transitions – have sufficient S/N and phases can be determined with relatively smaller errors. Figure 11(a) shows relation between the  $\phi_{off}$  and  $\phi_{on}$  for 12 such null transitions in the trailing component of PSR J1741–0840. For a complete stoppage of drifting,  $\phi_{off}$  and  $\phi_{on}$  should exhibit linear trend. It is clear from this comparison that there is no significant correlation between  $\phi_{off}$  and  $\phi_{on}$  – with cross-correlation coefficient less than 0.02. For PSR J1840–0840, on the contrary, we observed completely anti-correlated  $\phi_{off}$  and  $\phi_{on}$  (seen from Figures 12(a) and 13(a)). Implication of which are discussed further below.

Although nulling represents complete absence of any detectable emission, the charging and discharging of the polar gap may still be operating. If sub-pulses on the emission beam continue to drift – with similar or different rota-

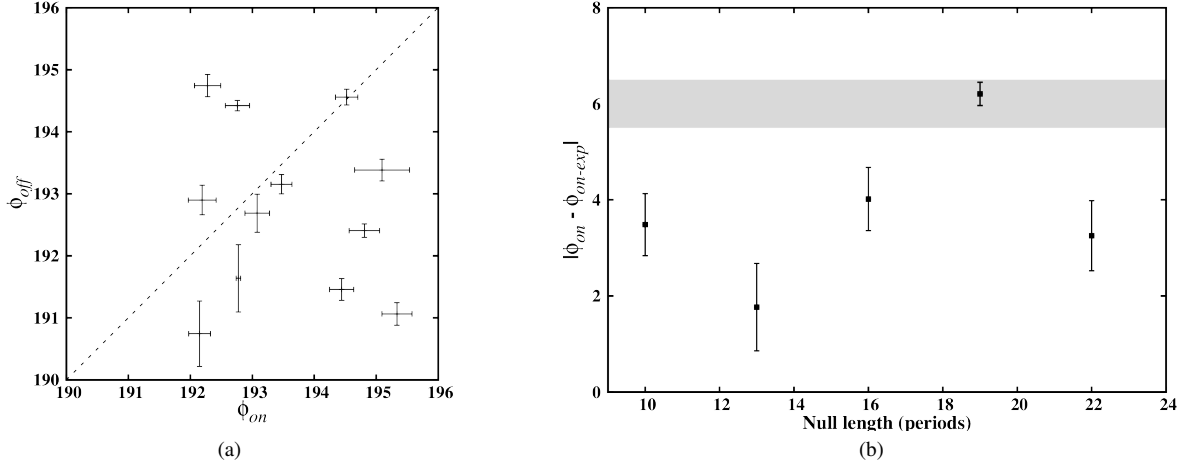


**Figure 11.** Comparison between the pulse phase across nulls for the trailing component of PSR J1741–0840 at 625 MHz. (a) The distribution of the turn-on phase versus the turn-off phase across nulls, and (b) absolute phase differences across the nulls as a function of null lengths. The shaded region in the right hand panel corresponds to the average width of the component with the errors. We binned the measured  $\Delta\phi$  into bins of five null lengths, shown here as filled squares corresponding to given null length bin, along with the corresponding error bars.

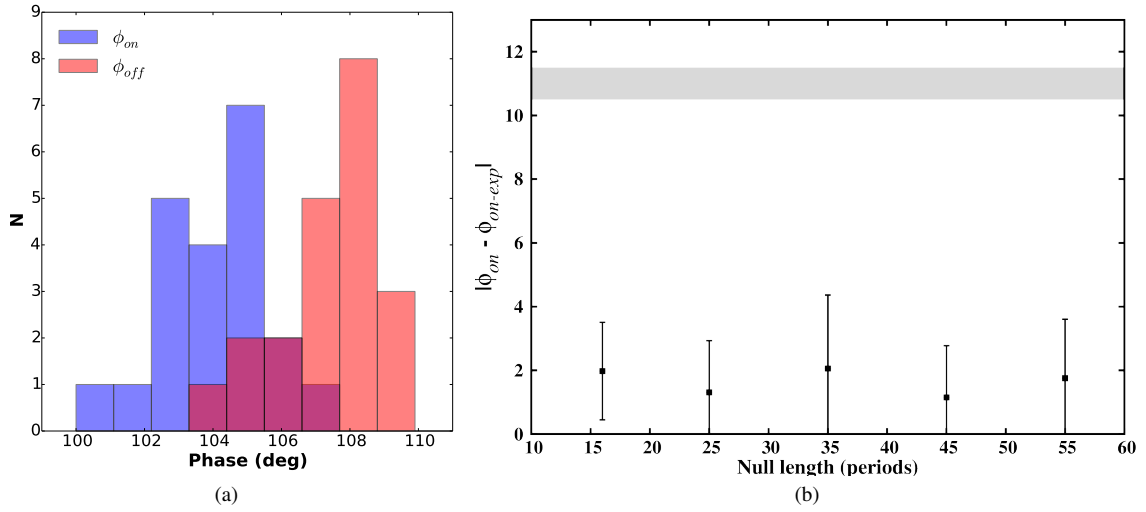


**Figure 12.** The relation between the turn-on and turn-off phases for the leading component of PSR J1840–0840 at 625 MHz. (a) Histograms of measured distribution of  $\phi_{on}$  and  $\phi_{off}$  which clearly show very distinct distribution suggesting peculiar preferences of burst pulse phase around nulls. (b) Absolute phase differences ( $\Delta\phi$ ) as a function of null lengths. The measured null-lengths were binned into seven bins and average  $\Delta\phi$  was measured for each bin. The shaded region in the right hand panel corresponds to the average width of the leading component with the errors.

tion speed – during the null state, the difference between the turn-on and the turn-off phases can be predicted based on the length of nulls. Furthermore, it is also likely that a pulsar retains memory of the turn-off phase only for certain length of nulls as in the case of PSR B0031–07 where only short nulls were shown to have such memory (Joshi & Vivekanand 2000). Thus, there are two scenarios that need to be tested, (a) drifting continues at its regular speed or (b) drifting slows down or speeds up during nulls. If drifting continues at its regular speed, it would be possible to predict location of the expected

turn-on phase ( $\phi_{on-exp}$ ) from Equation 1, given a  $\phi_{off}$ , length of the null (NL),  $P_3$ , and slope of driftband (D) before the null.

$$\phi_{on-exp} = \phi_{off} + \text{mod}(D \times NL, P_3) \quad (1)$$

Here, *mod* represents remainder from the drifting periodicity. If we find the  $\phi_{on-exp}$  to be outside the width of the component, we subtract the width of the corresponding component to truncate  $\phi_{on-exp}$  inside the component width window. In principle, the bounding limits for sub-pulse localization should come from measurement of  $P_2$ . However, for

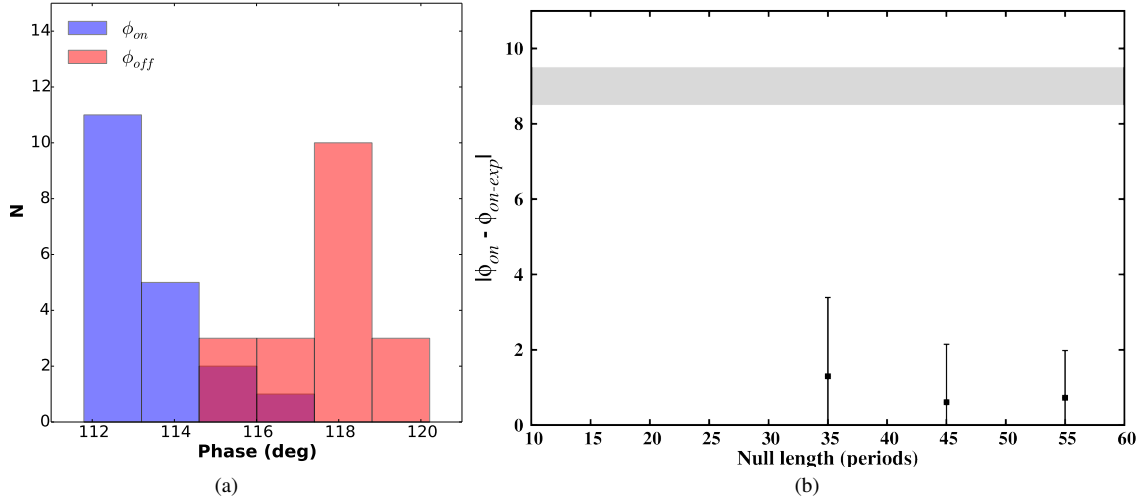


**Figure 13.** Similar relation between the turn-on and turn-off phases for the trailing component of PSR J1840–0840 at 625 MHz. (a) Histograms of measured distribution of  $\phi_{on}$  and  $\phi_{off}$  for the trailing component of PSR J1840–0840 at 625 MHz. The distribution clearly shows very distinct distribution suggesting peculiar preferences of burst pulse phase around nulls also occur in the trailing component. (b) Absolute phase differences ( $\Delta\phi$ ) as a function of null lengths. The measured null-lengths were binned into three bins and average  $\Delta\phi$  was measured for each bin. The shaded region in the right hand panel corresponds to the average width of the trailing component with the errors.

example, the leading component of PSR J1840–0840 has  $\hat{D}$  of around  $0.9^\circ \pm 0.4^\circ / P_1$  and  $P_3$  of around  $13.5 \pm 0.7$  periods, we can find that  $P_2$  would be  $12^\circ \pm 6^\circ$  which is equivalent to its width ( $11^\circ \pm 0.5^\circ$ ) with larger errors. Thus, we chose to use component widths as more suitable bounding limits here in our case. We calculated  $\phi_{on-exp}$  for a range of null lengths for both pulsars.

For PSR J1741–0840, the absolute phase differences between the expected and observed turn-on phase ( $\Delta\phi = |\phi_{on-exp} - \phi_{on}|$ ) is shown in Figure 11(b). If drifting continues at its regular speed with a memory of turn-off phase, one is likely to observe roughly zero  $\Delta\phi$  for a given null length. From Figure 11(b) it can be pointed out that drifting does not continue at its regular speed during the observed null lengths. If PSR J1741–0840 exhibits phase memory only for shorter nulls, we can expect to find smaller  $\Delta\phi$  for shorter nulls. However,  $\Delta\phi$  are almost equal to the width of the component across various null lengths without exhibiting any trends from shorter to longer nulls. Thus, it can be speculated that PSR J1741–0840 does not retain information regarding the turn-off phase or drifting slopes of burst pulses prior to nulls. The turn-on phases are also random and do not have any association with the turn-off phases as pointed out in the earlier section. Thus, we can speculate that PSR J1741–0840 either slows down or speeds up its sub-pulse drifting during the null state. However, it should be noted that the duration of our observations and sensitivity of single pulses were not sufficient (as is clear by the relative error bars in Figure 11(a)) to investigate this in detail. Higher sensitive and longer observations are required to investigate changes in the drift rate and its association with

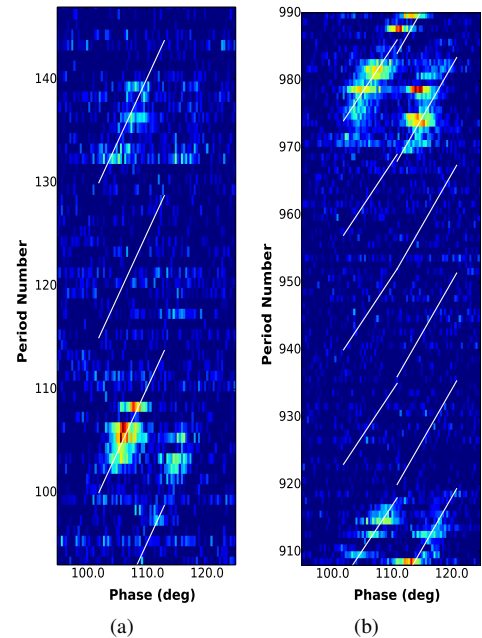


**Figure 14.** Examples showing speculative drifting during nulls for the leading and trailing components of PSR J1840–0840 at 625 MHz with (a) one missing driftbands (only shown for the leading component) and (b) three missing driftbands. The straight lines here are not fit to the driftbands in this case but are shown here just to illustrate approximate locations of the missing driftbands.

larger number of null transitions in this pulsar.

Contrary to PSR J1741–0840, when similar  $\Delta\phi$  were derived for the leading component of PSR J1840–0840, we

found remarkable similarities between the predicted and the measured turn-on phases. Figure 12(b) shows these  $\Delta\phi$  for various null lengths. We found that the  $\Delta\phi$  are significantly smaller than the width of the component and are located close to zero phase difference within the errors. Similarly, for the trailing component of PSR J1840–0840, we also found that the distribution of  $\Delta\phi$  is around zero phase difference (see Figure 13(b)). As noted earlier, the trailing component is relatively weak and sometimes does not provide good fits to the drift-rate slopes, thus we were able to measure the  $\Delta\phi$  for only eight transitions. These transitions were all came from mid to longer null lengths as shown in Figure 13(b). It should be noted that as  $D_l$  and  $D_r$  exhibit large spread in the measurements, we consider  $D_l$  and  $D_r$  before the onset of nulls and assume that they are constant across null states for the above calculations for the leading and trailing components, respectively. These assumptions may not be accurate for a few null states, which could explain the small spread from zero phase difference we see in Figures 12(b) and 13(b). Considering these small differences, these results still suggest that PSR J1840–0840 is likely to be among those pulsars that exhibit continuous drift in sub-pulses during nulls as it exhibits remarkable memory of its emission phase across the nulls in both of its profile components. Moreover, as pointed out in an earlier section, the turn-off phases are most likely to occur near the trailing-edge of component (end of driftband for positively drifting sub-pulses) and turn-on phases are likely to occur near the leading-edge of the component (start of the driftband for positively drifting sub-pulses). This leads to a speculation that, *is it likely that nulls in PSR J1840–0840 represent a complete absence of an entire driftband?*

Figures 14(a) and 14(b) show examples of two such null instances with missing one and three driftbands, respectively. An example of weak trailing component post short null can be seen in Figure 14(a) where making a true judgment regarding the turn-on phase was not possible. It should be noted that these examples shown here are just illustrations for possible locations of missing driftbands. The straight lines shown do not represent real fit to these driftbands. An additional confirmation regarding the missing driftbands can be considered from the measured null-length distributions shown in Figure 4(b). This distribution clearly shows an excess of around 12 to 18 period nulls which is equivalent to the drifting periodicities of  $13.5\pm 0.7$  periods for the leading component and  $18\pm 1$  period for the trailing component. This further supports our findings that most of the nulls in the leading and trailing components of PSR J1840–0840 are missing driftbands. However, these  $P_3$  measurements, as noted in Section 4, could easily be influenced by intervening nulls and thus may not be accurate. As the pulsar has long period and our sensitivity was limited we were only able to study this behavior for a handful of driftbands in PSR J1840–0840. Higher sensitivity and long observations are required to scrutinize it further for both components.

## 7. DISCUSSION AND CONCLUSIONS

We have reported nulling, drifting and their interactions in PSRs J1741–0840, and J1840–0840. Both pulsars clearly exhibit nulling and prominent drifting behaviors. A brief summary of our findings is listed in Table 2. For PSR J1741–0840 we estimate NF to be around  $30\pm 5\%$  while PSR J1840–0840 exhibits large nulling with NF of around  $50\pm 6\%$ . In a few nulling pulsars, it has been shown that the previously reported nulls are not true nulls. For example, PSR J1752+2359 appears to show weak single burst pulses during the null states which have significantly different polarization properties compared to the average profile (Gajjar et al. 2014b). In order to scrutinize any weak level emission during the observed nulls, we separated all the nulls and burst pulses for both pulsars. We did not find any detectable emission after combining all null pulses together for either pulsar. Thus, we can conclude that these nulls are true nulls and are not weak emission states (within the sensitivity limit of the observations).

### 7.1. Are different $P_3$ modes real?

We found that the trailing component of PSR J1741–0840 clearly exhibits driftbands while the leading component exhibits amplitude modulation without clearly exhibiting any drifting sub-pulses. We measured this amplitude modulation to be around  $4.9\pm 0.1$  periods for the leading component while the trailing component showed two distinct periodicities of around  $4.3\pm 0.1$  periods and  $4.6\pm 0.2$  periods. These measurements match with the previously reported periodicities for this pulsar (Weltevrede et al. 2006, 2007; Basu et al. 2016). In order to verify the different  $P_3$  modes, we measured periodicities for each consecutive and overlapping blocks of 356 pulses. We did not find any blocks that display dominating periodicity mode implying that these changes could occur on a smaller time-scale than the size of the block we have selected here. In order to scrutinize these changes, we measured slopes of driftbands which showed a very large spread around the mean value of  $1.1^\circ\pm 0.2^\circ/P_1$ . This spread was large enough to generate different  $P_3$  periodicities seen in PSR J1741–0840. Thus, we conclude that drifting in PSR J1741–0840 is very sporadic and it changes irregularly without clearly producing distinguishable drift modes.

Drifting in PSR J1840–0840 is very intriguing with relatively broad periodicity of  $13.5\pm 0.7$  periods in the leading component. The trailing component showed a broad  $P_3$  that peaks around  $18\pm 1$  periods. We noticed that these periodicities in either components are not stable and show large spread in the measured drift slopes. Although the distribution of D appears to be broad, we carried out *Hartigans' Dip test for Unimodality* and found that the distribution is still unimodal with high significance. In order to avoid small sample bias, we generated a range of slopes using Monte-Carlo simulation but did not find strong case for bi-modality. We measured the

average slope to be around  $0.9^\circ \pm 0.4^\circ / P_1$  and  $0.7^\circ \pm 0.4^\circ / P_1$  for the leading and trailing components in PSR J1840–0840, respectively. We can clearly see that the driftband slopes are relatively similar for both components in PSR J1840–0840 and the apparent difference seen in  $P_3$ , measured from LRFs, are likely originated from intervening nulls and sporadic nature of the driftband slopes. For example, the errors on  $D_l$  and  $D_t$  can easily produce this different  $P_3$  values when measured for a large number of driftbands. We also measured slopes of driftbands exclusively around the nulls for both pulsars but did not find their distributions to be significantly different from the general distributions for either pulsars. Thus, we conclude that PSRs J1741–0840 and J1840–0840 do not exhibit noticeable drift slope changes around nulls.

These results highlight an important point which should be noted that  $P_3$  is an average quantity which requires several pulses that follow similar repeating pattern. However, pulsars like PSRs J1741–0840 and J1840–0840 indicate that changes in the drifting pattern could occur on a much smaller time-scale (less than the size of a single driftband). Thus, measuring the slope of a driftband is essential to scrutinize any changes in the drifting pattern. Such study needs to be conducted for more drifting pulsars which exhibit different  $P_3$  and/or  $P_3$  modes between different profile components. In other words, the apparent  $P_3$  differences could simply be due to rapidly changing driftband slopes. Furthermore, [Basu et al. \(2016\)](#) have also suggested that in a few instances  $P_3$  measurements could cause ambiguity due to aliasing, which eventually hinders our understanding in connecting the observed behavior with the actual physical phenomena. Recently, [McSweeney et al. \(2017\)](#) also indicated that different  $P_3$  modes seen in PSR B0031–07 were actually gradual changes in the driftband slopes. Thus, we would like to emphasize that the different  $P_3$  needs to be scrutinized carefully by measuring changes in their driftband slopes as  $P_3$  could lead to incorrect interpretation of the physical changes.

### 7.2. On the origin of pulsar nulls

Among the various observed phenomena of radio pulsars, pulse nulling remains one of the most intriguing ones as no reasonable model has been able to explain the wide variety of observational features. Models such as temperature fluctuations to change coherence conditions ([Cheng 1981](#); [Deich et al. 1986](#)), switching between different gap discharge mechanisms ([Daugherty & Harding 1986](#); [Zhang et al. 1997](#); [Zhang et al. 1997](#)) and changes in the magnetospheric currents ([Timokhin 2010](#)) link pulsar nulling with the intrinsic magnetospheric changes. There are also other models which connect pulsar nulling with geometry of the pulsar beam ([Herfindal & Rankin 2007, 2009](#); [Rankin & Wright 2008](#)). The emission in the radio beam, as suggested by the [Ruderman & Sutherland \(1975\)](#), comes from localized regions (*aka.* sparks) on the polar cap. This notation was further investigated and a comprehensive model for subpulse drifting was suggested as

**Table 2.** A summary of results

PSR	J1741–0840	J1840–0840
Nulling Fraction (%)	30±5	50±6
Quasi-periodicity (periods)	33±4	–
Leading comp. $P_3$ (periods)	4.9±0.1	13.5±0.7
Trailing comp. $P_3$ (periods)	4.3±0.1 4.6±0.2	18±1
Leading comp. $\hat{D}$ ( $^\circ/P_1$ )	–	$0.9^\circ \pm 0.4^\circ$
Trailing comp. $\hat{D}$ ( $^\circ/P_1$ ) ...	$1.1^\circ \pm 0.2^\circ$	$0.7^\circ \pm 0.4^\circ$
$\phi_{on}$ leading comp.	–	103.9±0.2
$\phi_{off}$ leading comp.	–	106.9±0.1
$\phi_{on}$ trailing comp.	–	113.2±0.3
$\phi_{off}$ trailing comp.	–	117.7±0.2
$\Delta\phi$	$\sim W_c$	$\ll W_c$
Phase memory across nulls	No	Yes

Note : The  $\hat{D}$  represents average slopes while the  $\Delta\phi$  represents absolute phase difference between  $\phi_{on}$  and  $\phi_{on-exp}$  in term of width of the corresponding component ( $W_c$ ).

a rotating *carousel* of sub-beams ([Rankin 1993](#); [Deshpande & Rankin 1999](#); [Deshpande & Rankin 2001](#)). By treating the sub-beams as organized in an evenly spaced uniform pattern, [Herfindal & Rankin \(2007\)](#) argued that empty line-of-sight cuts or extinguished individual sub-beams are likely to repeat after certain pulsar periods thus giving rise to periodic nulling.

For PSR J1741–0840, we found a clear quasi-periodic fluctuation of around 33±4 periods in the burst bunching. Such quasi-periodic pattern in the occurrence of nulls have been reported in a few pulsars such as PSRs B0834+06 ([Rankin & Wright 2007](#)), B1133+16 ([Herfindal & Rankin 2007](#)), J1738–2330, and J1752+2359 ([Gajjar et al. 2014b](#)). This quasi-periodic bunching in PSR J1741–0840 can also be confirmed from its distributions of clustering of null-length and burst-length. The empty line-of-sight model also suggests that, as the sub-beams continue to drift during nulls, one would expect to predict the turn-on phase with high accuracy. In order to scrutinize drifting during nulls, we measured expected turn-on phase for nulls with various lengths for both pulsars. We found that PSR J1741–0840 does not seem to have any memory of the turn-off phase during the nulls as the absolute differences are comparable to the width of the component and did not show any trends for longer or shorter nulls. Furthermore, missing line-of-sight model can explain certain fraction of partial nulls – nulls seen in only one of the profile components ([Lyne & Ashworth 1983](#); [Vivekanand 1995](#); [van Leeuwen et al. 2002](#); [Janssen & van Leeuwen 2004](#)). In the case of PSR J1741–0840, we did not notice any partial nulls. Moreover, recent studies by [Gajjar et al. \(2012\)](#) and [Cordes \(2013\)](#) showed that nulling is inherently random and state transition from null-to-burst, and vice-verse, can be modeled by Markov chain models. [Cordes \(2013\)](#) further suggested that certain external influences acting with these random emission state transitions could mimic quasi-periodic energy fluctuations. Such influences may arise from an external

body (Cordes & Shannon 2008) or neutron star oscillations (Clemens & Rosen 2004) or near-chaotic switches in the magnetosphere's non-linear system (Timokhin 2010). Thus, based on lack of phase memory and partial nulls, we speculate that the missing line-of-sight model is less likely to produce the quasi-periodic feature seen in PSR J1741–0840.

We also studied preferences for turn-on and turn-off phases around nulls for both pulsars. For PSR J1741–0840 we did not find any peculiar preference for these phases. We also measured cross-correlation between the measured phases but did not notice any trends which might suggest a complete stop in drifting during nulls and resume from the same turn-off phase after nulls. However, for PSR J1840–0840 we found strong preferences for turn-on and turn-off phases which are significantly different from each other. It seems that, in most occasions PSR J1840–0840 tends to start nulling after what appears to be an end of a driftband for both components. Thus, most of the turn-off phases were found to occur near the trailing edge of a given component. Similarly, when the pulsar switches back to emission phase, in most occasions it starts at the beginning of a new driftband as most of the turn-on phases were found near the leading edge of both components. Such preferences have not been seen in any nulling-drifting pulsar to the best of our knowledge. Moreover, PSR J1840–0840 also showed a good match between the expected and measured turn-on phases which seems to suggest that it might continue to drift during nulls. Furthermore, PSR J1840–0840 also shows a good fraction of nulls with length similar to the length of a typical driftband. Thus, it is likely that nulling in PSR J1840–0840 is due to extinguishing sub-beams and empty line-of-sight passing over these sub-beams as proposed by Herfindal & Rankin (2007). If the above model is true for PSR J1840–0840, one would also expect to see partial nulls as both components are likely to be originating from the outer conal ring. However, both components seem to show simultaneous nulling as seen from the single pulses in Figure 1(b). However, we can not completely rule out missing line-of-sight model in this case due to lack of our knowledge in the localization of these components in the emission cone.

Assuming that PSR J1840–0840 does retain information regarding the phase of the last burst pulse, an alternative theory to missing line-of-sight model can be explored. This model of pulse nulling, first proposed by Filippenko & Radhakrishnan (1982), predicts a break in the two-stream instabilities which occurs during a steady polar gap discharge. Two-stream instabilities are produced due to the propagation of secondary particles with different momenta. These secondary particles are generated from the high-energy primary particles at initial gap discharge. A situation can occur for long period pulsars (like PSR J1840–0840) in which gap discharges, normally at roughly the same rate as the potential drop, would increase before the sparking. The polar cap then attains a steady discharge state in which no high-energy primary particles are produced for subsequent consecutive two-

stream instabilities and bunching. It can be speculated that, this steady state is reached after a buildup from the residual potential, which is a *left-over* from each gap discharge during normal non-steady condition (non-null state). Once the residual potential reaches the maximum gap height potential, the pulsar attains a steady state during which no radio emission is emitted (null state). However, the sparks could still be rotating on top of the polar cap. When the residual potential discharges, the pulsar resumes its normal interrupted sparking action that gives rise to primary particles with high energy for the consecutive bunching and coherence. The charging and discharging of this residual potential, in addition to the normal gap discharge, has an inherent memory associated with them. The time-scale of this memory mechanism should be higher for pulsars with long period and low surface magnetic field. PSR J1840–0840 here fits the criteria (see Table 1) for this mechanism to be operational which could be the reason we are seeing strong evidence of such phase memory during its nulls.

Although, we are able to demonstrate remarkable nulling and drifting interactions in PSR J1840–0840, more sensitive and longer observations would certainly provide intriguing details. Recently, the GMRT has been upgraded with the wider bandwidth of 200 MHz (Kumar 2014; Konar et al. 2016) which is much broader than 32 MHz used for our observations. Observations using such wider bandwidth will improve single pulse S/N by orders of magnitude and will allow us to robustly model both the components.

## 8. ACKNOWLEDGMENTS

We would like to thank the referee for very useful comments and suggestions. VG acknowledges the West Light Foundation of the Chinese Academy of Sciences project XBBS-2014-21. VG would also like to thank Bhal Chandra Joshi and Dipanjan Mitra for useful discussion regarding pulsar drifting in general. JPY supported by the Strategic Priority Research Program of the Chinese Academy of Sciences, Grant No. XD23010200. RY acknowledges supports from NSFC Project no. 11573059; the Technology Foundation for Selected Overseas Chinese Scholar, Ministry of Personnel of China; and the Joint Funds of the NSFC Grant No. U1531137. We thank the staff of the GMRT who made these observations possible. The GMRT is operated by the National Centre for Radio Astrophysics of the Tata Institute of Fundamental Research (NCRA-TIFR).

## REFERENCES

- Backer, D. C. 1970, *Nat.*, 228, 42
- Basu, R., Mitra, D., Melikidze, G. I., et al. 2016, *ApJ*, 833, 29
- Biggs, J. D. 1992, *ApJ*, 394, 574
- Biggs, J. D., McCulloch, P. M., Hamilton, P. A., Manchester, R. N., & Lyne, A. G. 1985, *MNRAS*, 215, 281
- Burke-Spolaor, S., Johnston, S., Bailes, M., et al. 2012, *MNRAS*, 423, 1351

- Camilo, F., Ransom, S. M., Chatterjee, S., Johnston, S., & Demorest, P. 2012, *ApJ*, 746, 63
- Cheng, A. F. 1981, in *IAU Symposium, Vol. 95, Pulsars: 13 Years of Research on Neutron Stars*, ed. W. Sieber & R. Wielebinski, 99–101
- Clemens, J. C., & Rosen, R. 2004, *ApJ*, 609, 340
- Cordes, J. M. 2013, *ApJ*, 775, 47
- Cordes, J. M., & Shannon, R. M. 2008, *ApJ*, 682, 1152
- Daugherty, J. K., & Harding, A. K. 1986, *ApJ*, 309, 362
- Deich, W. T. S., Cordes, J. M., Hankins, T. H., & Rankin, J. M. 1986, *ApJ*, 300, 540
- Deshpande, A. A., & Rankin, J. M. 1999, *ApJ*, 524, 1008
- Deshpande, A. A., & Rankin, J. M. 2001, *MNRAS*, 322, 438
- Esamdin, A., Lyne, A. G., Graham-Smith, F., et al. 2005, *MNRAS*, 356, 59
- Filippenko, A. V., & Radhakrishnan, V. 1982, *ApJ*, 263, 828
- Gajjar, V., Joshi, B. C., & Kramer, M. 2012, *MNRAS*, 424, 1197
- Gajjar, V., Joshi, B. C., Kramer, M., Karuppusamy, R., & Smits, R. 2014a, *ApJ*, 797, 18
- Gajjar, V., Joshi, B. C., & Wright, G. 2014b, *MNRAS*, 439, 221
- Hartigan, J. A., & Hartigan, P. M. 1985, *The Annals of Statistics*, 13, 70
- Herfindal, J. L., & Rankin, J. M. 2007, *MNRAS*, 380, 430
- . 2009, *MNRAS*, 393, 1391
- Hermsen et al. 2013, *Science*, 339, 436
- Hotan, A. W., van Straten, W., & Manchester, R. N. 2004, *PASA*, 21, 302
- Huguenin, G. R., Taylor, J. H., & Troland, T. H. 1970, *ApJ*, 162, 727
- Janssen, G. H., & van Leeuwen, J. 2004, *A&A*, 425, 255
- Joshi, B. C., & Vivekanand, M. 2000, *MNRAS*, 316, 716
- Konar, S., Bagchi, M., Bandyopadhyay, D., et al. 2016, *Journal of Astrophysics and Astronomy*, 37, 36
- Kumar, B. A. 2014, in *Astronomical Society of India Conference Series, Vol. 13, Astronomical Society of India Conference Series*, 457–460
- Lorimer, D. R. 2001, *Astronomical Research and Technology*, No. 2001
- Lorimer, D. R., Faulkner, A. J., Lyne, A. G., et al. 2006, *MNRAS*, 372, 777
- Lyne, A., Hobbs, G., Kramer, M., Stairs, I., & Stappers, B. 2010, *Science*, 329, 408
- Lyne, A. G., & Ashworth, M. 1983, *MNRAS*, 204, 519
- Manchester, R. N., Lyne, A. G., Taylor, J. H., et al. 1978, 185, 409
- McSweeney, S. J., Bhat, N. D. R., Tremblay, S. E., Deshpande, A. A., & Ord, S. M. 2017, *ApJ*, 836, 224
- Prabhu, T. 1997, MSc Thesis, IISc Bangalore, India, doi:10.1046/j.1365-8711.2000.03567.x
- Rankin, J. M. 1986, *ApJ*, 301, 901
- . 1993, *ApJ*, 405, 285
- Rankin, J. M., & Wright, G. A. E. 2007, *MNRAS*, 379, 507
- . 2008, *MNRAS*, 385, 1923
- Ritchings, R. T. 1976, *MNRAS*, 176, 249
- Ruderman, M. A., & Sutherland, P. G. 1975, *ApJ*, 196, 51
- Sobey, C., Young, N. J., Hessels, J. W. T., et al. 2015, *MNRAS*, 451, 2493
- Swarup, G., Ananthakrishnan, S., Kapahi, V. K., et al. 1991, *Current Science*, 60, 95
- Taylor, J. H., Manchester, R. N., & Huguenin, G. R. 1975, *ApJ*, 195, 513
- Timokhin, A. N. 2010, *MNRAS*, 408, L41
- van Leeuwen, A. G. J., Kouwenhoven, M. L. A., Ramachandran, R., Rankin, J. M., & Stappers, B. W. 2002, *A&A*, 387, 169
- van Leeuwen, A. G. J., Stappers, B. W., Ramachandran, R., & Rankin, J. M. 2003, *A&A*, 399, 223
- van Straten, W., Demorest, P., & Osłowski, S. 2012, *Astronomical Research and Technology*, 9, 237
- Vivekanand, M. 1995, *MNRAS*, 274, 785
- Vivekanand, M., & Joshi, B. C. 1997, *ApJ*, 477, 431
- Vivekanand, M., & Joshi, B. C. 1999, *ApJ*, 515, 398
- Wang, N., Manchester, R. N., & Johnston, S. 2007, *MNRAS*, 377, 1383
- Weltevrede, P., Edwards, R. T., & Stappers, B. W. 2006, *A&A*, 445, 243
- Weltevrede, P., Stappers, B. W., & Edwards, R. T. 2007, *A&A*, 469, 607
- Wen, Z. G., Wang, N., Yuan, J. P., et al. 2016, *A&A*, 592, A127
- Wright, G. A., & Fowler, L. A. 1981, *A&A*, 101, 356
- Zhang, B., Qiao, G. J., & Han, J. L. 1997, *ApJ*, 491, 891
- Zhang, B., Qiao, G. J., Lin, W. P., & Han, J. L. 1997, *ApJ*, 478, 313